ON THE EFFECT OF WIDTH DIRECTION THICKNESS VARIATIONS IN WOUND ROLLS

Z. HAKIEL

Eastman Kodak Company

Rochester, NY USA

ABSTRACT

A first order model has been developed, which predicts the widthwise variability in wound roll diameter and stresses. This model has been verified experimentally on wound rolls of film and qualitative agreement between the predicted and measured results was found. The theoretical model and experimental techniques used in its verification are described.

NOMENCLATURE

b	width of web
c (j)	widthwise outside core radius distribution, where j designates widthwise position
E	Young's modulus of the web in the length direction
EXC (x, y)	function defined as $EXC\ (x,y) = \begin{cases} x - y & for\ x > y \\ 0 & otherwise \end{cases}$
EXT (x, y, x^1, y^1, x^2, y^2,...)	polynomial extrapolation algorithm (5) for computing a new estimate of x corresponding to a function value y based on prior estimates x^1, x^2, ... and corresponding function values y^1, y^2, ...
h (j)	average widthwise thickness distribution, where j designates widthwise location
$\bar{h}$	average web thickness of web
IRSN	algorithm for prediction of in-roll stresses described in (4)
M	number of widthwise locations used in algorithm
MIN (x_1, x_2, x_3, ...)	function selects the smallest of a vector of values

N	number of laps in the wound roll
$P(i, j)$	interlayer pressure stress as defined in (4)
$r(i, j)$	widthwise distribution of radius to the inside surface of lap i, where j designates widthwise position
$R_o(i)$	relaxation radius for lap i; radius at which the lap would be stress free
$R_0^1, R_0^2, \ldots$	successive estimate of $R_o(i)$
$T(i, j)$	in-roll tension stress as defined in (4)
$T_a(i)$	actual winding tension force for lap i
$T_w(i)$	predicted winding tension force for lap i
ε_ω	circumferential winding tension strain in outer lap
$\rho(i\,j)$	widthwise roll radius distribution (roll profile), where i designates the lap number within the roll and j designates widthwise position
σ_ω	circumferential winding tension stress in outer lap

INTRODUCTION

An ideal web has uniform thickness in both the width and the length directions. Several in-roll stress models have been described in the literature for such ideal webs, e.g. (1)-(4). Real webs, as produced for example on extrusion casting machines, have thickness variations in both the width and the length directions. The width direction thickness variations in such webs tend to be persistent in the lengthwise direction. When webs with lengthwise-persistent widthwise thickness variations are wound, the resulting rolls tend to have hardstreaks, which are areas of increased roll radius and increased interlayer pressure.

Hardstreaks are undesirable, because they may lead to web imperfections. To understand the formation of hardstreaks, a simple extension of the in-roll stress model described in (4) has been developed and is described below. The new model predicts the widthwise variations in the outside roll radius (roll profile) and winding tension based on the widthwise thickness variations of the web, the mechanical properties of the web, and the nominal value of the winding tension. The model then employs the in-roll stress algorithm described in (4) to compute the in-roll stresses for widthwise segments of the roll, thus yielding approximate in-roll stress values as a function of the width and radial directions in the wound roll.

In order to verify the roll profile predictions obtained with the new model, an instrument was constructed which uses an LVDT sensor to traverse the width of the roll and determine the widthwise radius variations. In order to verify the in-roll stress predictions, a segmented core was constructed and instrumented with strain gages to permit interlayer pressure measurements to be made at the core at numerous widthwise locations. The roll profile instrument and the segmented core were used on 10-in wide rolls of PET film to verify predictions obtained with the new model and thus verify its validity.

THEORETICAL MODEL

Overview:

The objective of this model is to predict the widthwise variations in outside roll radius, winding tension, interlayer pressure, and in-roll tension in a roll wound of a web with lengthwise-persistent widthwise thickness variations. The model determines the widthwise winding tension distribution in a particular lap based on the widthwise distribution of the outside roll radius and the total winding tension in that lap. It then computes a new outside roll radius based on the widthwise thickness distribution of the web and the level of contact between the lap wound on and the roll. Once the widthwise distribution of tension is determined for all of the laps in the wound roll, the roll is "split-up" into independent widthwise segments for which the interlayer pressure and in-roll tension stresses are determined with the algorithm described in (4).

Key Assumptions:

In addition to the assumptions made in (4), the following key assumptions are made. First, in the prediction of the widthwise roll radius and winding tension distributions, the winding roll is assumed to be incompressible in the radial direction. Second, the web does not offer any resistance to bending. Lastly, there is very high friction between the lap being wound and the roll; i.e., the lap being wound cannot slide on the outside of the winding roll.

Derivation:

Consider a winding roll with a widthwise varying radius or roll profile $\rho(i-1, j)$, as is depicted in Fig. 1. Consider the winding of lap number i under total tension $T_a(i)$ onto that roll. This lap may or may not make full contact with the winding roll surface. In those areas where contact is made, the lap being wound on will assume the shape of the winding roll surface. In those areas where there is no contact, the web will be suspended as a straight cylindrical surface above the surface of the roll, as is depicted in Fig. 2.

Let us now define the widthwise distribution of the radius measured to the inside surface of lap i after it has been wound on as $r(i, j)$. If full contact is made between lap i and the roll, then we will simply have

$$r(i, j) = \rho(i-1, j) \qquad (1)$$

Now, let's consider the stresses and strains in the web which are in the plane of the web and which are implied by the radius distribution $r(i, j)$. The relationship between $r(i, j)$ and $\rho(i-1, j)$ in the case of partial contact between lap i and the roll is illustrated further in Fig. 2. Suppose $R_o(i)$ is a radius which corresponds to the inside radius of an unstretched lap of web. We call $R_o(i)$ the relaxation radius. Then in the case of partial contact between lap i and the roll we would have for lap i

$$r(i, j) = EXC\left(\rho(i-1, j), R_0(i)\right) \qquad (2)$$

For either the full or partial contact case, the circumferential tensile strain for lap i may be written as

$$\varepsilon_\omega = \frac{r(i,j) - R_0(i)}{R_0(i)} \tag{3}$$

Since we assumed that the web is unable to slide in the axial direction, we will have a circumferential stress, as given by

$$\sigma_\omega(i,j) = \frac{E}{1-\nu^2}\left\{\frac{r(i,j) - R_0(i)}{R_0(i)}\right\} \tag{4}$$

By summing the circumferential stress across the width of the web, we obtain an expression for the predicted winding tension force in the outer lap

$$T_\omega(i) = \sum_{j=1}^{M}\left\{\sigma_\omega(i,j)\frac{\bar{bh}}{M}\right\} = \frac{E\bar{bh}}{M(1-\nu^2)}\sum_{j=1}^{M}\left\{\frac{r(i,j) - R_0(i)}{R_0(i)}\right\} \tag{5}$$

This predicted value must of course equal the actual tension force value, in order to preserve equilibrium in the outer lap of the winding roll

$$T_\omega(i) = T_a(i) \tag{6}$$

We are now in a position to determine the value of the relaxation radius R_0 if the outside roll radius distribution $\rho(i-1, j)$ is known. We begin by guessing a value of R_0. We then determine if we have full contact between the lap being wound on and the roll surface by use of the criterion

$$\text{If } R_0(i) \le \text{MIN}\{\rho(i-1,j)\} \rightarrow \textbf{full contact} \tag{7}$$

Once we determine the nature of the contact between the outer lap and the roll, we use equation (1) or (2) to compute r(i, j) . We then proceed to evaluate the predicted winding tension using (5) and check to see if equation (6) is satisfied within some error tolerance. If (6) is not satisfied, we generate a new guess for R_0 and repeat the above procedure. For the third and subsequent iterations, we can apply polynomial extrapolation to improve our guesses for R_0 . After several iterations, we will have a value of R_0 which will cause (6) to be satisfied within a specified tolerance.

In order to apply the above procedure to a winding roll with an unknown radius distribution, we start out by setting the roll radius distribution equal to the known or assumed core radius distribution for the first lap

$$\rho(0,j) = c(j) \tag{8}$$

We then apply the above procedure to compute r(1,j) and $R_0(1)$.

Subsequently, we compute a new roll radius distribution by adding the widthwise thickness distribution

$$\rho(1,j) = r(1,j) + h(j) \tag{9}$$

We then repeat the above procedure for the third and subsequent laps until all of the laps have been added.

Once the predicted widthwise radius distributions have been calculated for all of the laps, winding tension stress distributions can be computed by using (4). Then, we can "split-up" the roll into independent widthwise segments and compute the average winding tension for each of those segments. We subsequently can use this winding tension information to compute the in-roll stresses with the algorithm described in (4).

The computational scheme described above is further illustrated in the flowchart of Fig. 3.

EXPERIMENTS

Roll Profile Measurement:

Roll profile, as, defined above, is the widthwise distribution of the outside winding roll radius. An instrument for measuring roll profile was constructed and is shown in Fig. 4. It consists of a carriage-mounted LVDT for sensing the radius nonuniformities. This carriage traverses, the roll width on two rods. A potentiometer-based displacement transducer is connected to the carriage to measure the widthwise position of the LVDT. This permits the recording of roll radius variations as a function of width on an X-Y recorder. The entire carriage and rod assembly is mounted on a larger carriage which rides in the radial direction, thus permitting measurement of the roll profile to be made at various roll radii. The LVDT selected for this instrument is air loaded and generates a contact force of approximately 0.5 ounce. This light loading does not appear to deform the surface of the roll being measured significantly.

Interlayer Pressure Measurement:

In order to measure the widthwise variations of interlayer pressure, a segmented-instrumented core was constructed. This core is capable of measuring the interlayer pressure at the core in one-inch widthwise segments. The core which was constructed for these experiments was a 5-in diameter aluminum core consisting of twelve independent 1-in-wide segments. Each of the segments in this core is instrumented with two strain gages which measure the circumferential contraction of the segment. All of the segments are mounted on a common inner core by means of rubber "O-rings" and are pinned to the inner core with three pins. This allows the segments to contract radially independently of each other and of the inner core. It also allows torque to be transmitted from the inner core to the segments and on to the winding roll. The inner core also houses all of the cables coming from and going to the strain gages on the segments as well as the connector to which these cables are attached. Temperature compensation strain gages are also mounted on one of the end plates of the inner core. A photograph of the segmented-instrumented core is shown in Fig. 5.

Pressure readings are obtained with the segmented-instrumented core once the roll becomes stationary and a cable to connected from the core to a signal conditioner/readout. Readings are sequentially obtained for each of the segments via

a selector switch. In order to verify the predicted relationship between the strain level in the core segments and pressure on the core, a calibration fixture was built and utilized. This fixture consists of a metal vessel which slips over the core and which contains a rubber tube inside. To calibrate the core, the fixture is slipped over the core and the tube is inflated with a gas at a known pressure. The gain of the signal conditioner can then be adjusted to give readouts of pressure equal to the air pressure in the rubber tube.

Verification Experiments:

In the verification experiments, two 10-inch-wide webs of 4-mil PET were wound on the segmented-instrumented core at two levels of winding tension: 2 lb/in and 4 lb/in. The rolls were wound at the low speed of 125 fpm in order to minimize the effects of air entrainment on in-roll stresses. During the winding of each of the rolls, the winder was stopped several times with the web tension maintained in the machine, so that measurements of roll profile and pressure at the core could be performed.

Once the winding experiments were completed, samples were cut from the two PET webs, so that widthwise thickness measurements could be made. Thirty equally spaced widthwise thickness traces were made for each of the webs using a contacting thickness gage interfaced with a data acquisition system. The thirty traces were then averaged in the lengthwise direction to obtain average widthwise thickness traces for each web.

RESULTS AND DISCUSSION

The average widthwise thickness traces obtained for the two PET webs used in the verification experiments are shown in Figures 6 and 7. From the thickness data, the nominal winding tension values used in the experiments, and previously measured mechanical properties for the PET webs, predicted roll profiles and widthwise winding tension distributions were obtained with the model described above. The measured roll profiles obtained for each of the rolls wound are shown alongside the predicted roll profiles for comparison in Figures 8 through 11.

From a comparison of the measured and predicted roll profiles, it may be seen that there is qualitative agreement between the measured and predicted results. The amplitude of the predicted hardstreaks tends to be somewhat higher than the amplitude of the measured ones. The shape of the predicted roll profiles generally follows the shape of the measured roll profiles quite well. The model does tend to exaggerate the abrupt changes in the profiles. This may be due in part to the assumption of no bending stiffness for the web in the current model. Any distortion which the LVDT sensor might induce in the portions of the roll which do not exhibit layer-to-layer contact would contribute to this effect as well.

For both of the webs used in the experiment, the measured and predicted roll profiles tend to roughly follow the shape of the average widthwise thickness distribution. It appears that during winding, in those areas where the thickness of the web is low, contact between laps in the roll is not made and the roll profile in those areas is flat. In those areas where the thickness is high, contact between laps in the roll does occur and hardstreaks or peaks appear in the roll profile. If there are many such high spots in the average thickness profile, the winding tension becomes distributed over a number of hardstreaks and none of them is very severe. However,

if there are only a few areas in the widthwise thickness distribution which are significantly higher than the rest of the web, severe hardstreaks will develop in those areas.

Predicted widthwise winding tension values obtained with the model for the experimental rolls were averaged over ten 1-inch-wide segments, which correspond to the ten segments of the segmented-instrumented core over which these rolls were wound. From the averaged predicted winding tension values and the properties listed in Table 5, predicted interlayer pressure values were obtained for each of the segments with the model. The values of pressure at the core taken from the predicted pressure distributions are plotted as a function of widthwise position in Figures 12 through 15. The measured values of core pressure for all of the segments in all of the rolls wound are given for several values of roll radius in Tables 1 through 4. The measured core pressures for all of the segments in the fully wound rolls are shown in Figures 12 through 15 along with the predicted values. The core pressure values which would exist in the rolls of PET if the thickness of the web were perfectly uniform and no hardstreaks were present were also calculated with the model for comparison and are included in Figures 12 through 15 as well.

From the plots of the measured and predicted core pressure values shown in Figures 12 through 15, it may be seen that agreement between the measured and predicted values is fairly good. This indicates that the model described above successfully predicts the widthwise variations in winding tension and interlayer pressure at the core due to widthwise variations in web thickness. It is also quite evident that the interlayer pressure at the core varies considerably in the widthwise direction for all of the rolls. This variation in core pressure can in fact be greater than one order of magnitude, as can be seen there.

SUMMARY & CONCLUSIONS

A model for computing widthwise variations in roll radius and in-roll stresses caused by widthwise web thickness variations was described. The model was verified on two rolls of PET film with the use of a roll profile measurement instrument and a segmented-instrumented core. It was shown that rolls with hardstreaks have interlayer contact in parts of the rolls only. Hardstreak severity was found to be dependent on the winding tension level and the number and amplitude of widthwise thickness variations of the web. It was found for the rolls used in the experiments that the actual maximum interlayer pressure in the rolls was significantly higher than the pressure which would have been predicted for a uniform roll.

REFERENCES

1. Altmann, H.C., Tappi 51(4); (1968)
2. Pfeiffer, J.D., Tappi 62(10); (1979)
3. Yagoda, H.P., J. Appl. Mech. 47; (1980)
4. Hakiel, Z., Tappi 70(5); (1987)
5. Press, W.H., et al, Numerical Recipies The Art of Scientific Computing, Cambridge 1988

TABLE 1

Measured core pressures in each of the ten segments of web A wound with a tension of 2 lb/in to the outside radius indicated.

RADIUS (in)	PRESSURE FOR SEGMENT # (psi) 1	2	3	4	5	6	7	8	9	10
2.8	30	26	59	48	44	30	9	9	10	12
3.0	48	39	107	91	74	54	34	9	10	12
3.3	61	48	154	135	97	71	36	10	12	13
3.8	73	61	232	216	133	92	48	12	13	14
4.8	76	76	331	318	175	109	50	12	13	14
6.0	78	99	425	410	215	122	55	15	16	18
7.5	79	121	507	486	248	130	56	17	19	20

TABLE 2

Measured core pressures in each of the ten segments of web A wound with a tension of 4 lb/in to the outside radius indicated.

RADIUS (in)	PRESSURE FOR SEGMENT # (psi) 1	2	3	4	5	6	7	8	9	10
2.8	87	89	130	112	109	94	83	55	53	50
3.0	148	150	234	213	193	177	146	78	64	59
3.3	201	201	336	318	271	251	194	88	65	60
3.8	279	282	498	490	401	365	265	94	64	58
4.8	378	405	747	766	617	542	376	100	63	56
6.0	450	526	971	1005	813	697	481	106	64	54
7.5	512	657	1190	1231	1008	855	585	118	71	59

TABLE 3

Measured core pressures in each of the ten segments of web B wound with a tension of 2 lb/in to the outside radius indicated.

RADIUS (in)	PRESSURE FOR SEGMENT # (psi)									
	1	2	3	4	5	6	7	8	9	10
2.8	13	18	39	41	32	28	36	21	27	19
3.0	13	23	48	52	39	49	63	48	40	27
3.3	13	23	48	55	41	68	99	90	51	35
3.8	13	23	50	57	43	92	150	151	65	45
4.8	16	26	52	59	48	132	230	241	82	52
6.0	18	27	54	60	52	163	296	317	96	55
7.5	19	30	55	62	57	194	363	395	114	57

TABLE 4

Measured core pressures in each of the ten segments of web B wound with a tension of 4 lb/in to the outside radius indicated.

RADIUS (in)	PRESSURE FOR SEGMENT # (psi)									
	1	2	3	4	5	6	7	8	9	10
2.8	58	62	88	87	80	81	98	81	85	71
3.0	90	104	137	144	130	157	191	174	153	130
3.3	105	128	166	186	169	232	293	275	219	191
3.8	112	139	181	220	210	338	439	425	320	283
4.8	113	141	187	250	280	521	684	671	481	418
6.0	112	140	189	265	350	686	894	881	625	529
7.5	117	146	195	282	430	839	1078	1061	765	641

TABLE 5

Properties Used as Model Inputs

Core Diameter	5.0 inch
Wound Roll Diameter	15.0 inch
Web Thickness	0.004 inch
Young's Modulus	629,200 psi
Stack Modulus	Exponential Function: $C_0\left(1-e^{\frac{pressure}{c_1}}\right)$ $C_0 = 361762.7$ psi $C_1 = 1254.2$ psi
Poisson's Ratio	0.01
Core Modulus	512,500 psi
Winding Tension	2 lb/in and 4 lb/in (constant)

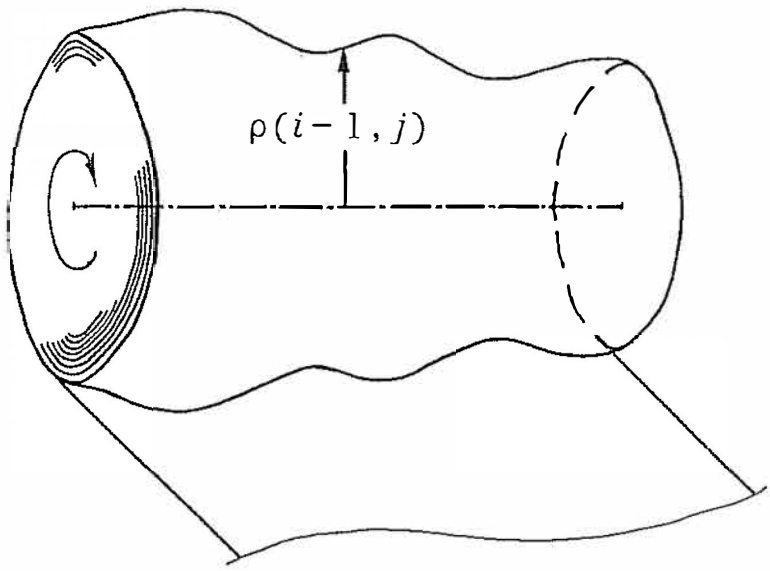

Figure 1 Exaggerated view of the widthwise roll radius distribution or roll profile for a roll with i - 1 laps wound on

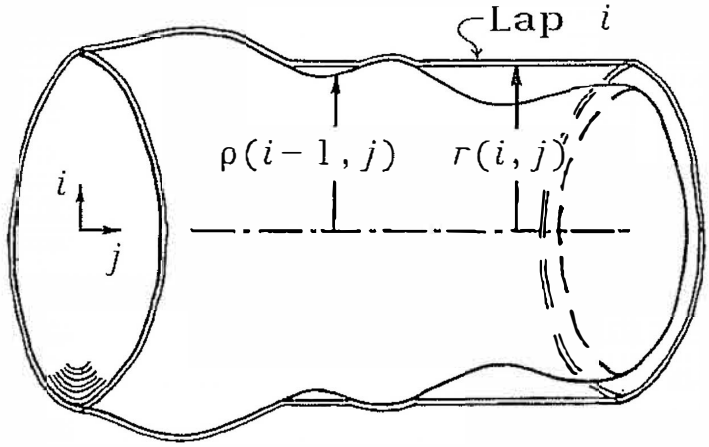

Figure 2 Exaggerated view of the relationship between the widthwise roll radius distribution r (i,j) and the roll profile ρ (i- 1, j) for a roll with partial contact between laps i and i- 1

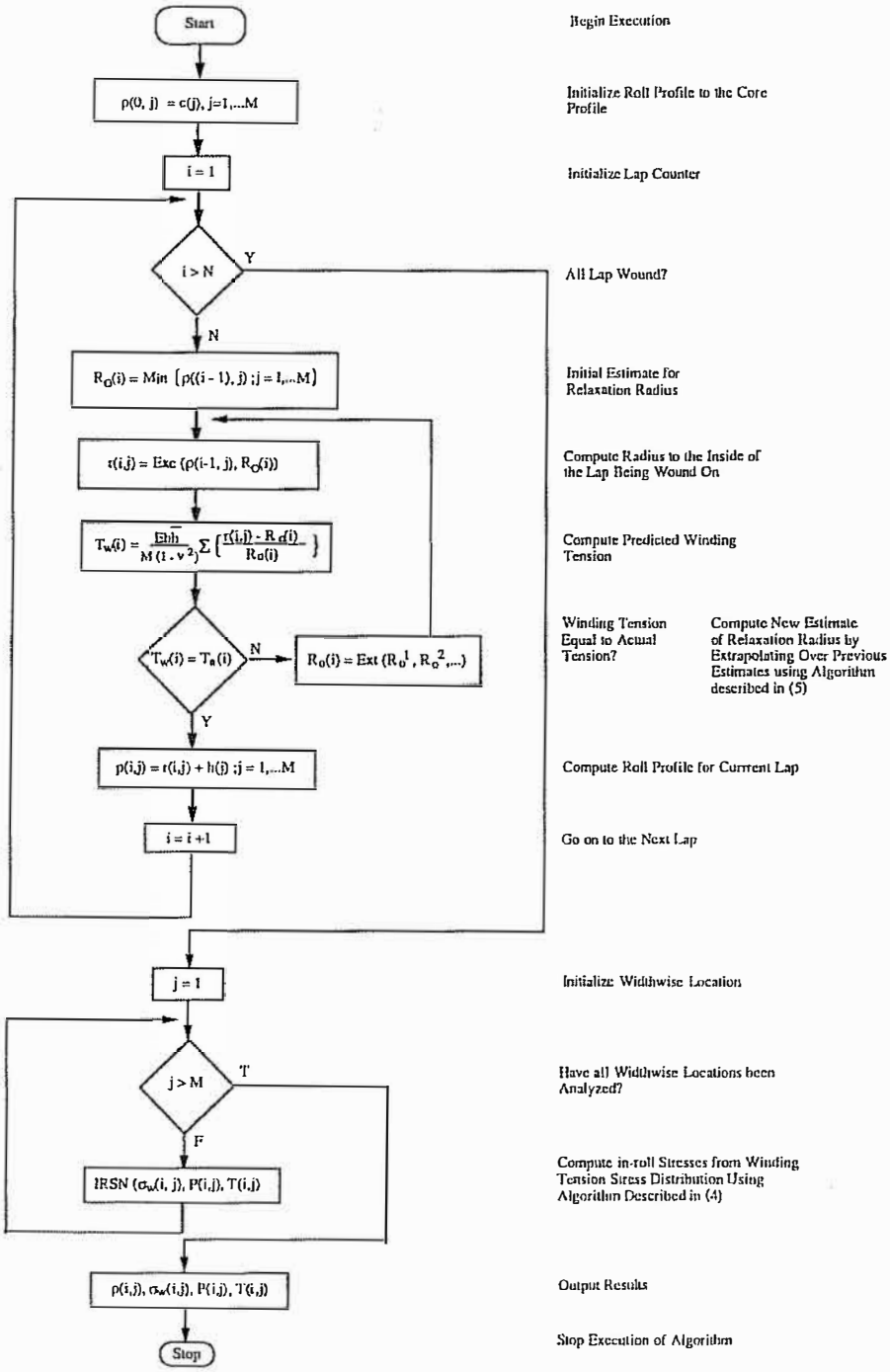

Figure 3 Flowchart of algorithm for computing roll profile and in-roll stresses

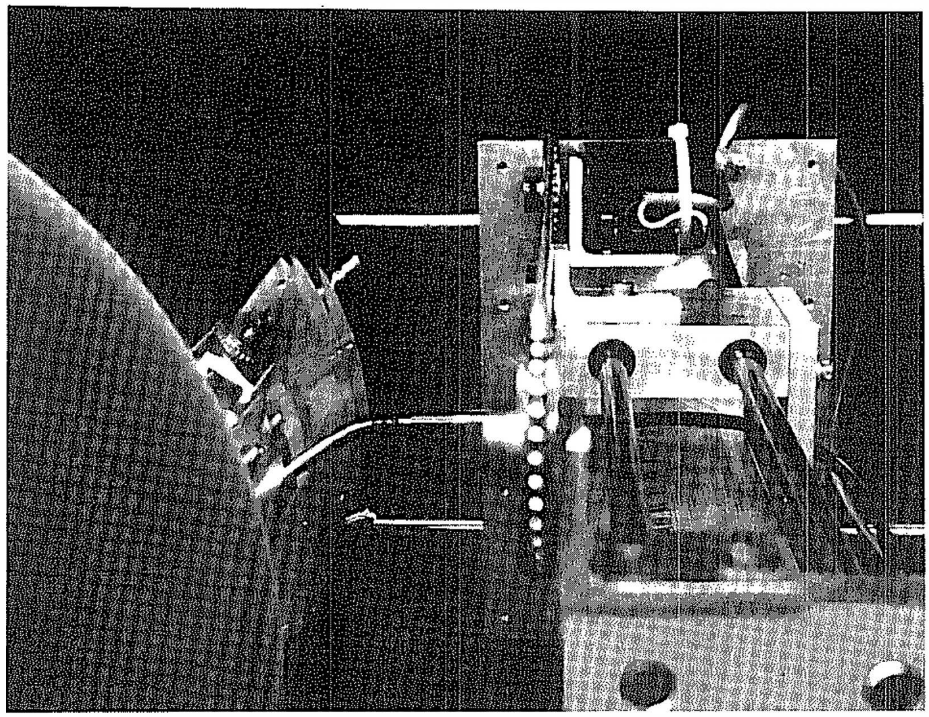

Figure 4 Photograph of roll profile measurement instrument

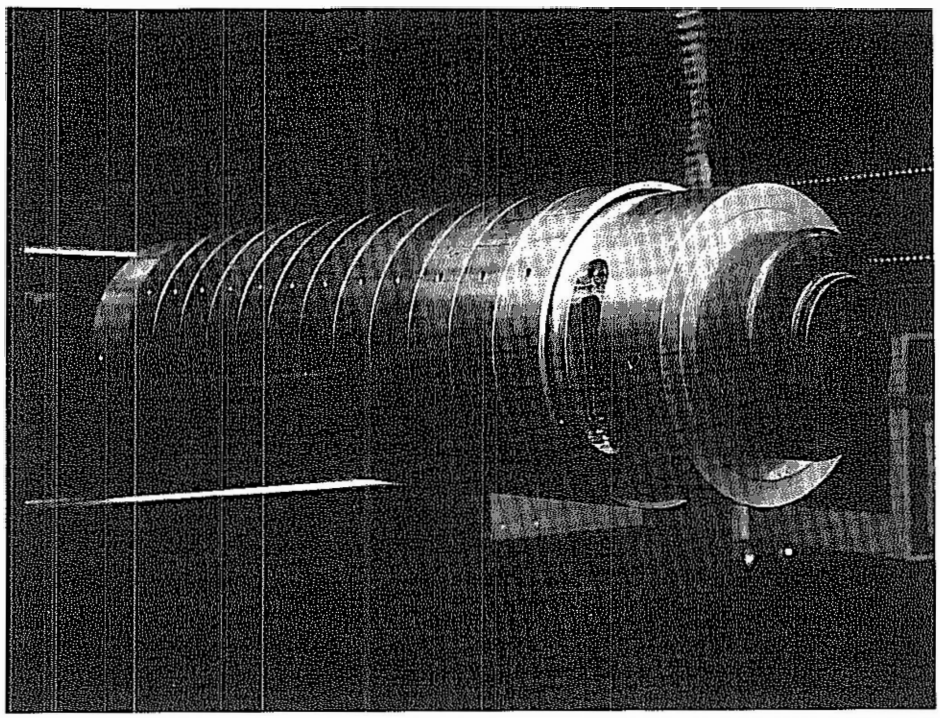

Figure 5 Photograph of segmented-instrumented core

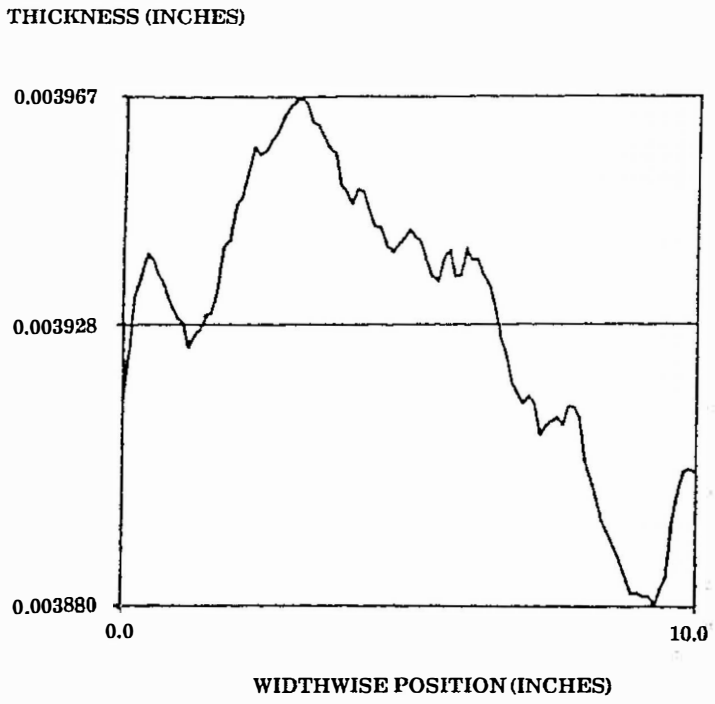

Figure 6 Average widthwise thickness trace for roll A

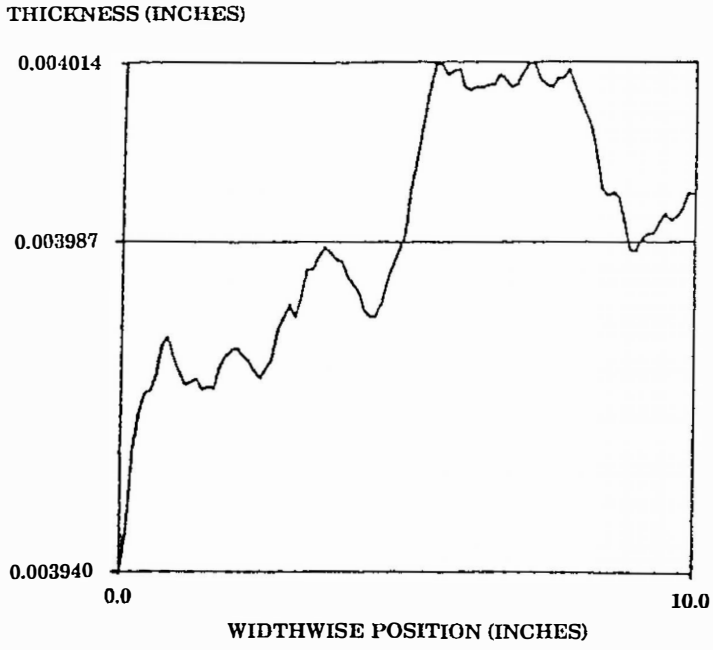

Figure 7 Average widthwise thickness trace for roll B

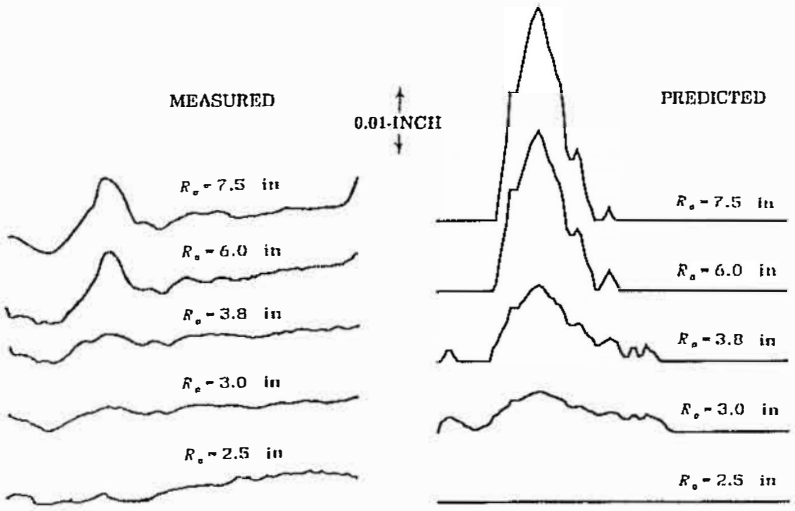

Figure 8 Measured and predicted roll profiles for roll A wound with a tension of 2 lb/in

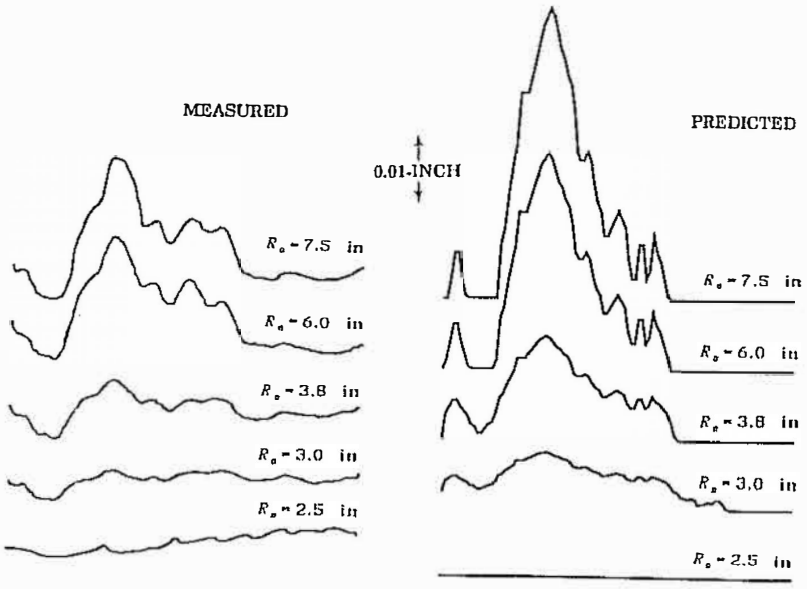

Figure 9 Measured and predicted roll profiles for roll A wound with a tension of 4 lb/in

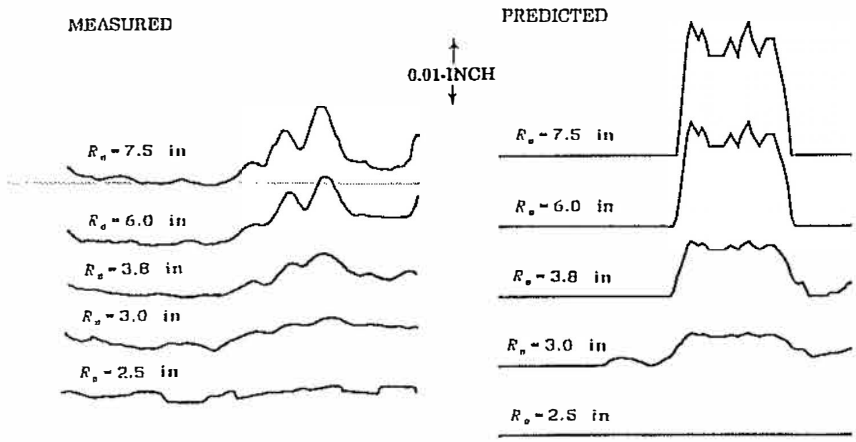

Figure 10 Measured and predicted roll profiles for roll B wound with a tension of 2 lb/in

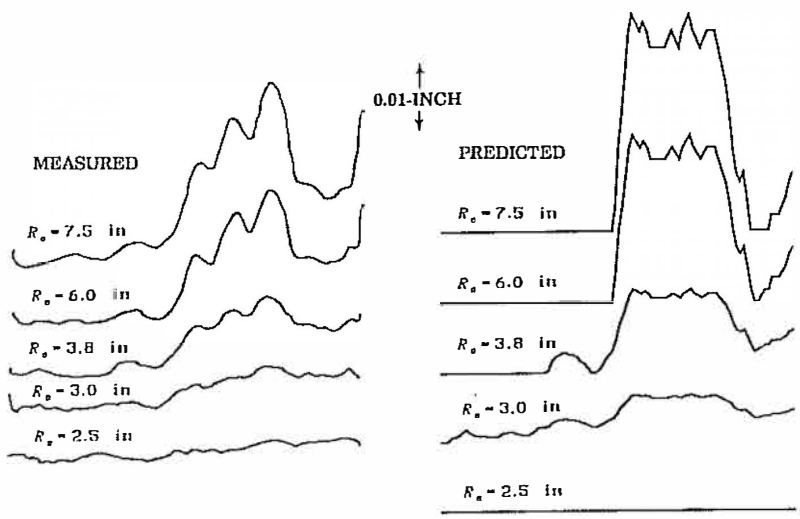

Figure 11 Measured and predicted roll profiles for roll A wound with a tension of 4 lb/in

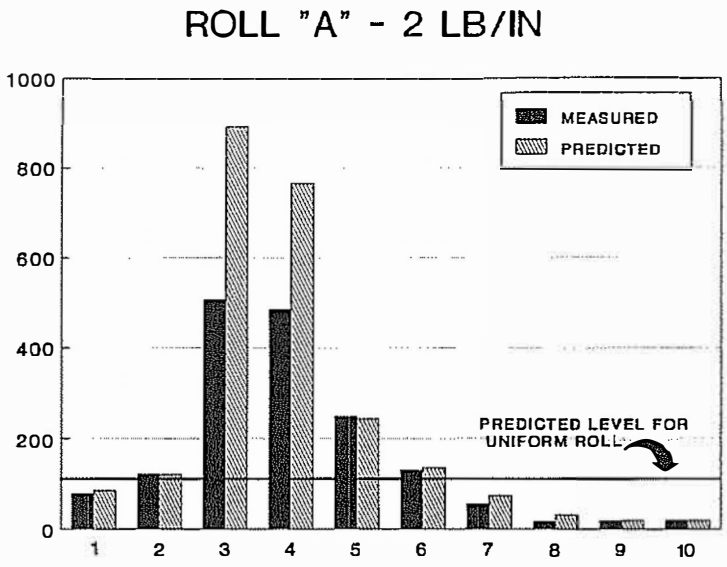

Figure 12 Measured and predicted core pressure (psi) for roll A wound with a tension of 2 lb/in as a function of widthwise location (in)

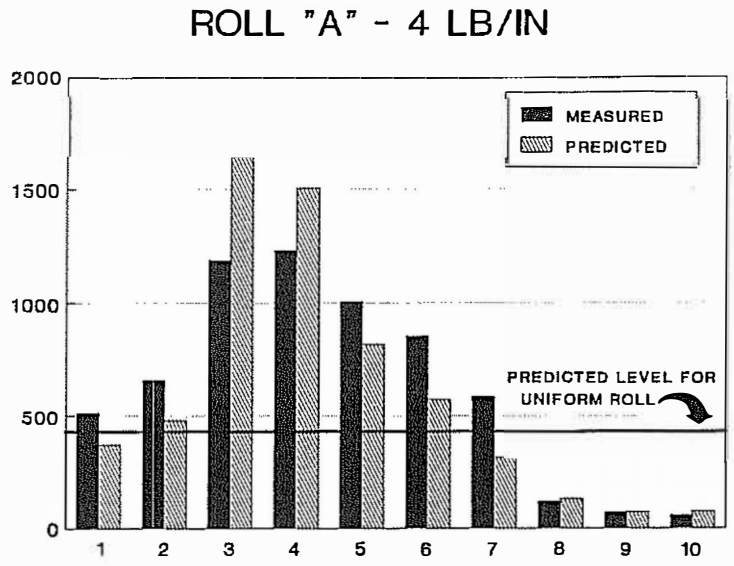

Figure 13 Measured and predicted core pressure (psi) for roll A wound with a tension of 4 lb/in as a function of widthwise location (in)

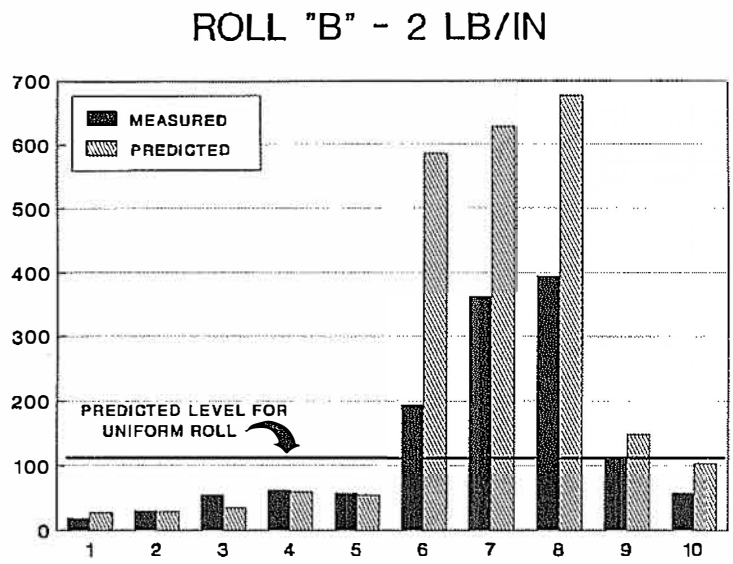

Figure 14 Measured and predicted core pressure (psi) for roll B wound with a tension of 2 lb/in as a function of widthwise location (in)

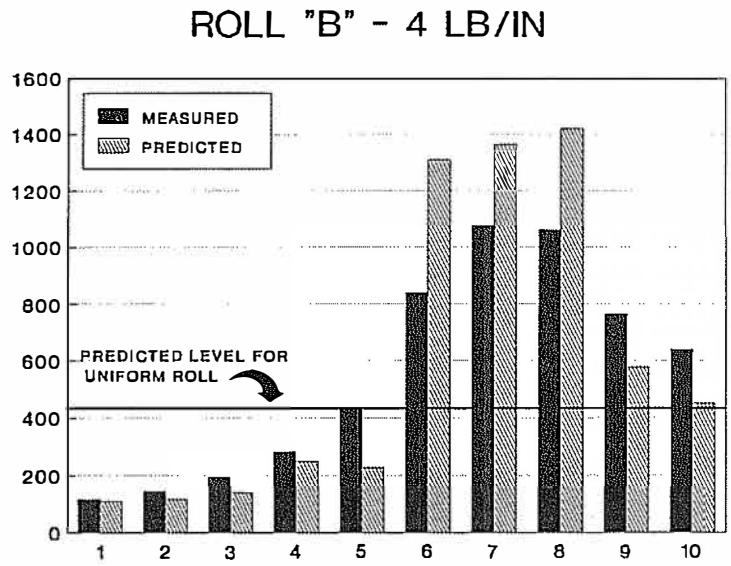

Figure 15 Measured and predicted core pressure (psi) for roll B wound with a tension of 4 lb/in as a function of widthwise location (in)

What computer capacity is required to solve this type of problem?
Robert Lucas, Beloit Corporation

Both, the one-dimensional in-roll stress problem and the widthwise distribution of tension problem could be solved on a P.C. If you couple the two problems together you need a large computer and a lot of CPU time.

To what extent are the necessary arrays stored within RAM or on hard disk memory?
Robert Lucas, Beloit Corporation

Again there are two answers depending upon which version you are dealing with. In the simpler version the arrays are really not all that large because you really don't need to retain all the information. It also very much depends on how many widthwise locations you are analyzing. If you only have 10 as I did in this example then it is a manageable array, but obviously you can play games and put things on hard disk and so on.

What is computational time?
Robert Lucas, Beloit Corporation

I couldn't tell you; it's a few seconds on an IBM mainframe

How was the segmented mandrel instrumented?
Bob Reuter, Sandia

There were strain gauges mounted on the inside of the aluminum rings and the aluminum rings were attached to the inner core by way of pins which allowed torque to be transmitted between the two but allowed the outer rings to contract radially. So the answer is that they were instrumented with strain gauges on the inside coupled with some additional strain gauges for temperature compensation. It's described I think in the paper.

What did you assume for the radial modulus of the PET film in carrying out the calculations?
Dilwyn Jones, ICI

I don't remember that off the top of my head but I could provide that information for the final copy of the paper. That was a measured value that we actually obtained on the specimen. (See Table 5)

What calibration technique was used for segment core strain gages?
Tim Walker,3M

Actually it turned out that we didn't require any but we did use some for verification. We built a pressure vessel which consisted of an aluminum container with a rubber bladder on the inside that was blown up with air. That was used to verify the calibration of the strain gauges. Actually just from a prediction of what strain you would get for the thin aluminum shells you can actually get a direct measurement of what the pressure is. You don't really need to calibrate that but we did just to verify the predictions.

Have the roll examples been wound with contact roll (nip)?
Andre Thill, Mobil

No we looked at center winding only.

Could you comment on the compression effects on radius, at different crossweb pressures? What about softer materials such as paper?
Ron Swanson,3M

That's a real good question. One of the underlying assumptions of the model is that in the outer lap analysis we are assuming the roll to be incompressible in the radial direction. So that if the material was highly compressible radially that assumption obviously would break down and we couldn't use this approach. That's where marrying the two loops that I described, I think, would help in that you could actually go through, compute the outer lap solution and actually do the internal stress analysis, compute the amount of radial deflection and add that to the roll profile. It can be done. We have done it. It is very computationally intensive and for the film examples that we considered it really wasn't necessary, but I think for paper it probably would be.